SMALL-SCALE VARIABILITY OF OROGRAPHIC PRECIPITATION IN THE ALPS: CASE STUDIES AND IDEALIZED SIMULATIONS FOR THE NATIONAL PARK BERCHTESGADEN AREA

Günther Zängl

Meteorologisches Institut der Universität München, Munich, Germany
E-mail: *guenther@meteo.physik.uni-muenchen.de*

Abstract: High-resolution numerical simulations have been conducted to investigate the small-scale precipitation variability in the National Park Berchtesgaden area (southeastern Bavaria), which has the highest density of operational raingauge stations in the whole Alps. Part of the simulations have been conducted with realistic analysis data, considering two heavy-precipitation cases that occurred in July and August 2005. Both cases featured quite an unusual precipitation pattern, with a station lying on the southwestern flank of a major mountain massif receiving precipitation amounts far exceeding all surrounding stations in both cases. Despite some quantitative differences, the real-case simulations reproduce the observed precipitation pattern reasonably well. They indicate that the small-scale variability is dominated by the classical seeder-feeder mechanism. In addition, a number of semi-idealized simulations has been performed, combining realistic topography with synthetic large-scale flow conditions. Their goal is to investigate of the factors controlling the small-scale precipitation variability. It is found that the ambient wind direction has the largest impact on the small-scale precipitation patterns, followed by the wind speed and the location of the freezing level.

Keywords: *Small-scale precipitation patterns, seeder-feeder mechanism, high-resolution numerical modelling*

1. INTRODUCTION

There have been many studies on small-scale precipitation variability in mountainous terrain, either related to the seeder-feeder mechanism (Bergeron, 1965) for stable orographic lifting or to orographically triggered convection (e.g. Cosma et al., 2002; Kirshbaum and Durran, 2005). Unfortunately, current raingauge networks are not dense enough to fully resolve this variability, particularly in mountainous regions where stations are usually clustered at easily accessible valley locations. For convective precipitation, radar measurements can fill this gap to a large extent, but the situation is not as good for seeder-feeder-induced variability because the related precipitation enhancement is usually concentrated to fairly low elevations above ground and thus is difficult to detect with operational radar measurements. The main goal of this study is to examine to what extent high-resolution numerical simulations are able to generate realistic small-scale precipitation patterns, which could afterwards be used for a spatial interpolation of point measurements such as needed for climatologies or hydrological modelling. The present work focuses on the National Park Berchtesgaden in southeastern Germany, the region with the densest operational raingauge network in the whole Alps. Here, two heavy-precipitation cases (10–12 July 2005 and 15–17 August 2005) are examined that were characterized by a fairly unusual small-scale rainfall distribution. The real-case simulations are complemented by a number of semi-idealized simulations, combining realistic topography with idealized large-scale flow conditions. The outline of this paper is as follows. The setup of the simulations is described in section 2, followed by a discussion of the model results in section 3.

2. MODEL AND SETUP

The numerical simulations presented here have been conducted with the Penn State University / National Center for Atmospheric Research mesoscale model MM5, version 3.6 (Grell et al. 1995). Four two-way nested model domains are used with a horizontal mesh size of 16.2 km, 5.4 km, 1.8 km and 600 m, respectively. The area covered by the coarsest domain (domain 1) is displayed in Fig. 1 including the positions of the nests. Vertical resolution is provided by 39 unevenly spaced σ-levels, the lowermost one being about 15 m above ground. To allow for a realistic description of the relevant physical processes, a complete set of physics parameterizations for cloud microphysics, subgrid-scale convection, radiation and boundary-layer processes is used. With respect to microphysics, it has to be mentioned that the Reisner-Thompson scheme (Thompson et

al., 2004) is used for the July case (hereafter case 1) whereas the Goddard scheme (Tao and Simpson, 1993) is used for the August case (case 2) because these schemes yielded the highest skill scores in the respective case (not discussed here). The Goddard scheme is also used for the semi-idealized simulations. The initial and boundary conditions used for the real-case simulations are obtained from operational ECMWF data. The simulations start at 00 UTC 10 July 2005 and 12 UTC 15 August 2005, respectively, and are conducted for 54 h and 42 h, respectively. For the semi-idealized simulations, synthetic large-scale fields are prescribed as shown in Fig. 2. Two different temperature profiles are considered, starting from a sea-level temperature of 285 K and 275 K, respectively. The lapse rate depends on pressure and is kept slightly below the moist adiabatic one, and the relative humidity is set to 98% in the lower and middle troposphere. The ensuing profiles of equivalent potential temperature (θ_e) are shown in Fig. 2a. The wind profiles are characterized by positive vertical shear and a clockwise turning with height (Fig. 2b,c). The clockwise turning, corresponding to warm-air advection via the thermal wind relation, is used as a simple way to enforce large-scale lifting. This turned out to be important for obtaining realistic precipitation patterns. The wind direction will be referred to by its value at 700 hPa (360° in Fig. 2c) in the remainder of this paper. It will be varied between 315° and 30° and appears in the simulation name together with the acronyms given in Fig. 2 for the temperature and wind profiles (see caption of Fig. 4).

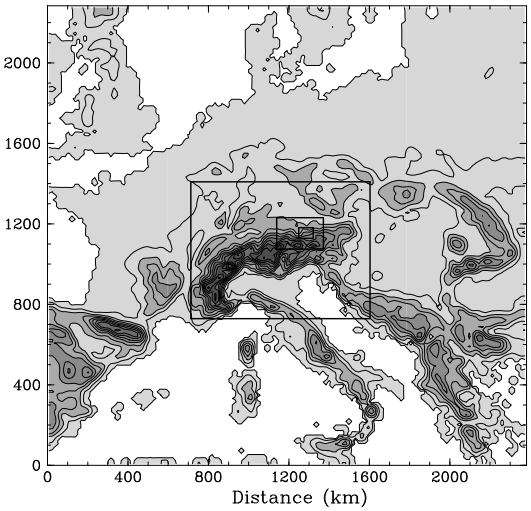

Figure 1: Topography of the first model domain (contours and shading with increments of 250 m and 500 m, respectively) and position of the nested domains (boxes).

3. RESULTS

3..1 Real-case experiments

The most striking feature of the observed precipitation fields (Fig. 3a,b) is a pronounced precipitation maximum at a station located on the southwestern flank of a major mountain massif (the Untersberg massif near Salzburg), far exceeding the values recorded at all surrounding stations. Apart from that, there is a tendency for higher rainfall accumulations at the inner-Alpine stations than close to the northern edge of the Alps, particularly in case 1 (Fig. 3a). The simulations reproduce the primary precipitation maximum at the Untersberg massif, but its magnitude is underpredicted in case 1 (Fig. 3c) and overpredicted in case 2 (Fig. 3d). A closer

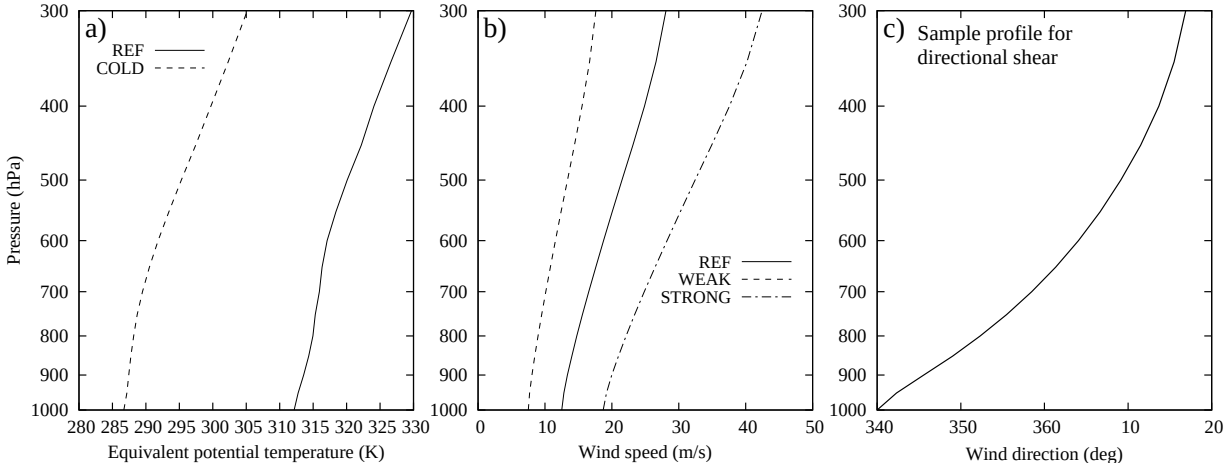

Figure 2: Profiles of (a) equivalent potential temperature, (b) geostrophic wind speed and (c) geostrophic wind direction used for the idealized simulations. (c) refers to a 700-hPa wind direction of 360°.

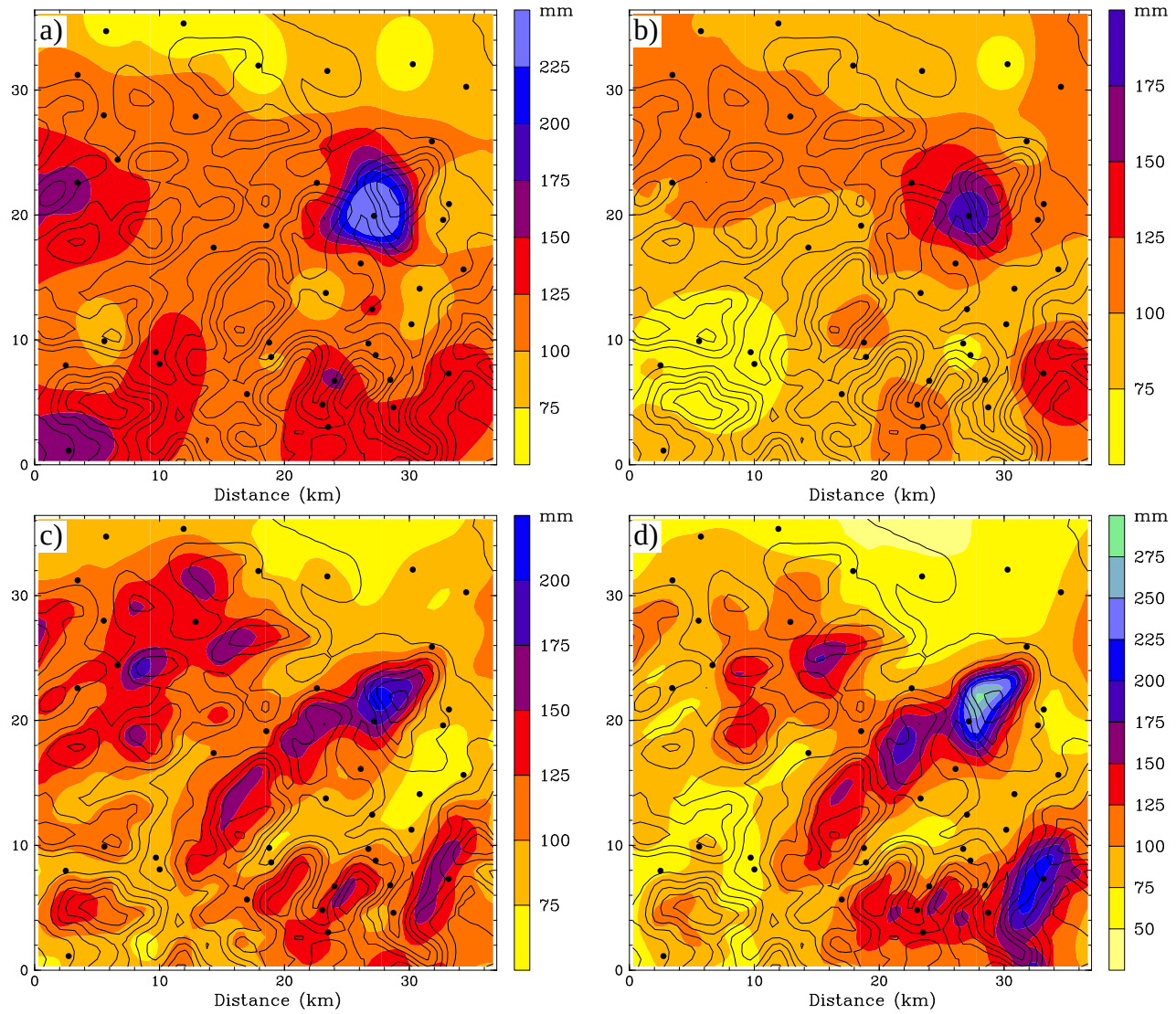

Figure 3: Accumulated precipitation fields in the analysis domain for 0600 UTC 10 July – 0600 UTC 12 July 2005 (left column) and 1800 UTC 15 August – 0600 UTC 17 August 2005 (right column). Model topography is contoured every 400 m, and black dots indicate raingauge stations. The upper (lower) panels show interpolated observed (simulated) precipitation.

analysis of the model results revealed that these maxima are generated by the classical seeder-feeder mechanism, combined with downstream advection of the precipitation hydrometeors. On average over the whole domain, the canonical correlation coefficient between simulated and observed precipitation amounts is 0.73 for case 1 and 0.71 for case 2.

3..2 Semi-idealized experiments

To obtain further information on the factors controlling the small-scale variability patterns, semi-idealized simulations have been conducted. The REF temperature and wind profiles (Fig. 2a,b) have been specified such as to approximately match those observed in the real cases. The real 700-hPa wind direction was about 30° in case 1 and 15° in case 2. The precipitation fields obtained from the semi-idealized simulations are shown in Fig. 4, accumulated over 24 h of simulation and scaled to a domain-average value of 100 mm (which is close to what occurred in the real cases). The patterns obtained for 700-hPa wind directions of 15° and 30° (Fig. 4b,c) are indeed fairly similar to those from the real-case simulations for case 2 and case 1, respectively, whereas a completely different pattern is obtained for 315° (run 315-REF, Fig. 4a). This indicates that the ambient wind

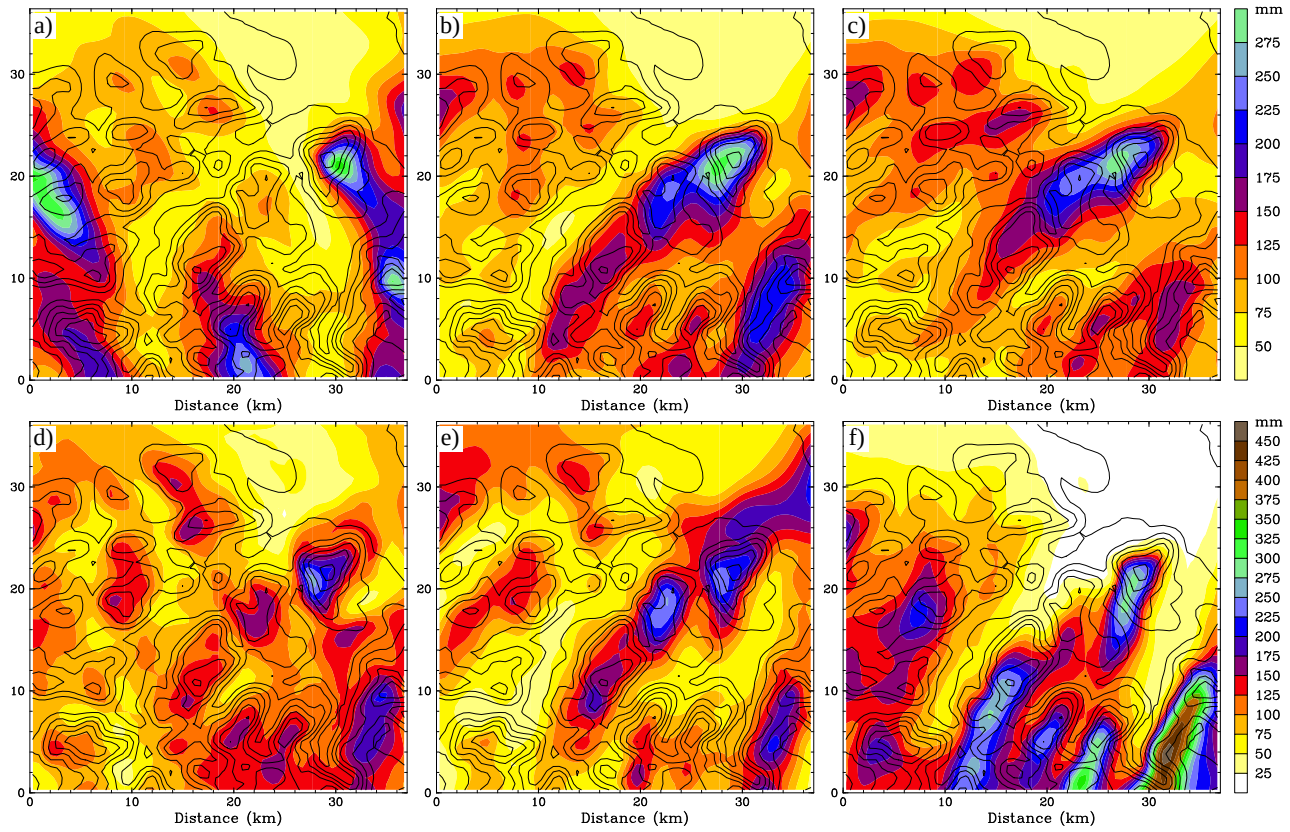

Figure 4: Accumulated precipitation (04-28 h) for the idealized simulations (a) 315-REF, (b) 015-REF, (c) 030-REF, (d) 015-COLD, (e) 015-WEAK and (f) 045-STRONG. All precipitation fields are scaled with a constant factor to obtain an average amount of 100 mm in domain 4A.

direction plays an important role in setting up the small-scale rainfall patterns. Changing the temperature or the wind speed has a smaller but still substantial impact. Specifically, decreasing the temperature by about 10 K ("COLD" in Fig. 2a) decreases the magnitude of the major precipitation peaks (Fig. 4d, cf. with Fig. 4b), and there are some moderate structural changes due to the lower freezing level. The general decrease of the precipitation amount (by a factor of about 2.4) does not appear in Fig. 4 due to the above-mentioned scaling. Decreasing the ambient wind speed (Fig. 4e, 015-WEAK) also reduces the local peaks and leads to relatively more precipitation near the northern edge of the Alps, whereas increasing the ambient wind (Fig. 4f, 015-STRONG) increases the peaks and shifts the precipitation into the interior of the Alps due to a stronger downstream advection of the hydrometeors. The correlation between the precipitation fields of 015-REF and 030-REF and the real-case data turned out to be similar as for the corresponding real-case simulations. Changing the ambient flow conditions strongly degrades the correlation, particularly for wind direction.

REFERENCES

Bergeron, T. 1965. On the low-level redistribution of atmospheric water caused by orography. *Suppl. Proc. Int. Conf. Cloud Physics,* Tokyo, May 1965, 96–100.

Cosma, S, Richard E, Miniscloux, F. 2002. The role of small-scale orographic features in the spatial distribution of precipitation. *Quart. J. Roy. Met. Soc.,* **128,** 75–92.

Grell, G. A., J. Dudhia, and D. R. Stauffer, 1995: A description of the fifth-generation Penn State/NCAR mesoscale model (MM5). NCAR Tech. Note NCAR/TN-398+STR, 122 pp.

Kirshbaum, D. J., and D. R. Durran, 2005. Observations and modeling of banded orographic convection. *J. Atmos. Sci.,* **62,** 1463–1479.

Tao, W-K, Simpson, J. 1993. Goddard cumulus ensemble model. Part I: Model description. *Terrestrial, Atmospheric and Oceanic Sciences*, **4,** 35–72.

Thompson, G, Rasmussen, RM, Manning, K. 2004: Explicit forecasts of winter precipitation using an improved bulk microphysics scheme. Part I: Description and sensitivity analysis. *Mon. Wea. Rev.,* **132,** 519–542.